GSA Data Repository 2019181

Murch, A.P., White, J.D.L., and Carey, R.J., 2019, Unusual fluidal behavior of a silicic magma during fragmentation in a deep subaqueous eruption, Havre volcano, southwestern Pacific Ocean: Geology, https://doi.org/10.1130/G45657.1

Supplemental Material

DR 1 Methods

Samples were taken from the caldera floor, walls and rims (Fig. 1) using ROV Jason and employing push-cores, scoops and vacuum-like 'slurp' samplers. A push core is a 3.5" diameter plastic tube open at one end that is designed to be inserted into sediment, then retrieved. A scoop is a frame holding both a fine (200 µm) and coarse (1 mm) netting layers, on a metal rod, intended to be dragged through the sediment to sample. Vacuum sampling uses a pump to draw in sediment with excess water is released through a >1 mm mesh and a 1000-200 µm fabric filter. Despite the range in sampling methods employed no discernible difference in the grainsize characteristics of samples taken by different methods has been identified.

All samples were immediately dried either in an oven at 90 ^{o}C or under an array of heat lamps for at least eight hours. Whole samples were hand sieved onshore, from -4 φ to 4 φ (from 16 mm to 0.063 mm) in ½ φ steps. The fraction remaining in each sieve was weighed on an electronic scale with 0.01-gram resolution.

Grain morphology and microtextures were investigated using secondary electron (SE) and back-scattered electron (BSE) methods on a Zeiss Sigma VP® Field-Emission-Gun Scanning Electron Microscope at the University of Otago. For SE (morphological) imaging, grains were mounted on an SEM stub using carbon tape and then carbon coated. BSE imaging was undertaken on grains mounted on a carbon coated polished briquette. In both cases, imaging was undertaken using a 15 keV accelerating voltage and a working distance of between 7.1 to 9.5 mm.

Secondary electron imaging was initially employed to conduct visual description of particles features diagnostic of fragmentation mechanism and define morphology componentry classes. Following this SEM SE montage image maps of samples were collected to conduct more quantitative examination of morphology componentry class distribution. Systematic creation of montaged maps was undertaken on 12 representative samples of S1 and S2 from various locations and depositional environments around the caldera. Image maps were collected of grain fractions 3 φ (125 µm), 4 φ (63 µm), and smaller than 4 φ (63 µm) in size. Point counting was then undertaken on the SEM SE montaged image maps, using a step size approximately 1.5 times the average grain size. At each point the grain was grouped by its morphology into one of three secondary morphological subgroups; Angular, Curvi-planar, and Fluidal. Point counting was undertaken until at least 400 points had been grouped, for each size fraction, or the grains had run out.

DR 2 Results of the SEM componentry for seafloor samples containing >75% S1/S2

	Fluidal			**Angular**			**Curvi-planar**		
Grain size (φ)	3	4	5	3	4	5	3	4	5
HVR159 Base	12.93	21.41	11.84	11.49	12.98	18.18	75.57	65.60	69.98
HVR159 Bulk	19.62	9.21	7.18	12.26	15.99	19.96	68.12	74.80	72.85
HVR132	11.98	14.44	4.34	6.69	16.61	17.83	81.34	68.95	77.83
HVR272	18.10	6.22	4.10	1.86	7.82	13.41	80.05	85.97	82.50
HVR134 Bulk	10.66	12.89	3.43	24.45	27.65	29.74	64.89	59.46	66.83
HVR031	15.20	16.82	5.62	9.45	9.55	21.20	75.36	73.64	73.19
HVR105	18.56	19.36	4.85	14.13	17.40	44.80	67.31	63.24	50.35
HVR122	35.34	10.10	9.13	12.37	15.40	26.94	52.30	74.49	63.93
HVR124	13.25	7.41	3.83	13.49	15.90	22.46	73.25	76.69	73.71
HVR191	25.38	27.88	10.10	16.41	10.22	26.12	58.21	61.90	63.78
HVR229	19.17	23.35	15.73	10.63	5.79	10.67	70.21	70.86	73.60
HVR283	26.35	20.37	8.45	10.80	8.41	18.07	62.85	71.21	73.48
Average	*18.88*	*15.79*	*7.38*	*12.00*	*13.64*	*22.45*	*69.12*	*70.57*	*70.17*
Max	*35.34*	*27.88*	*15.73*	*24.45*	*27.65*	*44.80*	*81.34*	*85.97*	*82.50*
Min	*10.66*	*6.22*	*3.43*	*1.86*	*5.79*	*10.67*	*52.30*	*59.46*	*50.35*
Giant pumice granulate	5.48	3.57	1.84	82.13	74.00	49.72	12.39	22.43	48.45

DR 3 Granulating the giant pumice

The Giant Pumice granulate was produced during this study using a mortar and pestle. Prior to the following procedure the mortar and pestle were thoroughly cleaned to remove dust and any fragments of previous uses. A fragment of Giant Pumice (GP) was place in the mortar at room temperature. The pestle was then used to attempt to crush the fragment placing a roughly vertically downward force. The GP fragment did not disintegrate however ash size fragments were produced at the base and top of the GP fragment where it was in contact with the mortar and pestle, respectively. Ash was likely produced by a combination of friction with the mortar and pestle and compression.

The generated ash was then collected. A fine brush was used to remove all fine the particles. The generated ash was then sieved in 1 φ steps. Following this SEM SE montage image maps were collected for extracts of the 3 φ (125 µm), 4 φ (63 µm), and smaller than 4 φ (63 µm) grain size fractions. Point counting was conducted on the SEM SE montaged image maps, using a step size approximately 1.5 times the average grain size. At each point the grain was grouped by its morphology into one of three morphological groups; Angular, Curvi-planar, and Fluidal. Point counting was undertaken until at least 400 points had been grouped, for each size fraction, or the grains had run out. The results of the point counting are presented in DR2.

DR 4 Magma viscosity and its effect on particle rounding

Sample	Giant pumice (Carey, et al., 2018)
SiO_2	71.92
TiO_2	0.47
Al_2O_3	14.01
Fe_2O_3	3.38
MnO	0.12
MgO	0.67
CaO	2.58
Na_2O	5.14
K_2O	1.62
P_2O_5	0.08
LOI	1.27
Total	*99.71*
H_2O total (wt%)	1
Temperature	**Log Viscosity (Pa s)**
750 ^oC	$10^{8.1}$
850 ^oC	$10^{6.7}$
950 ^oC	$10^{5.6}$
1050 ^oC	$10^{4.7}$

Whole rock major element chemistry data for the giant pumice from (Carey, et al., 2018), along with the viscosity range calculated for a range of temperatures. The approximate saturation water content is used for a vent of 900 mbsl (Newman and Lowenstern, 2002). Viscosity calculations undertaking using the methods of (Giordano et al., 2008).

The approximate timescale of particle rounding by surface tension (T_r) has been calculated using equation (10) from Wadsworth *et al.* (2017) for Havre ash with diameters of 1, 0.1, and 0.01 mm.

$$T_r = \frac{R\mu}{\Gamma}$$

Where R is the particle radius, μ is the magma viscosity, and Γ is the melt vapor interfacial tension here assumed to be 0.3 N m^{-1} (Gardner and Ketcham, 2011). Particle rounding timescales calculated for a range of eruption temperatures are compared with particle quenching timescales. Particle quenching rate was calculated using a lower end cooling rate of $10^{3.9}$ K s^{-1} from (Helo et al., 2013). The time taken for a particle to cool from a range of temperatures to a fixed glass transition point of approximately $10^{11.4}$ Pa s (Gottsmann et al., 2002) ~600 °C was then calculated.

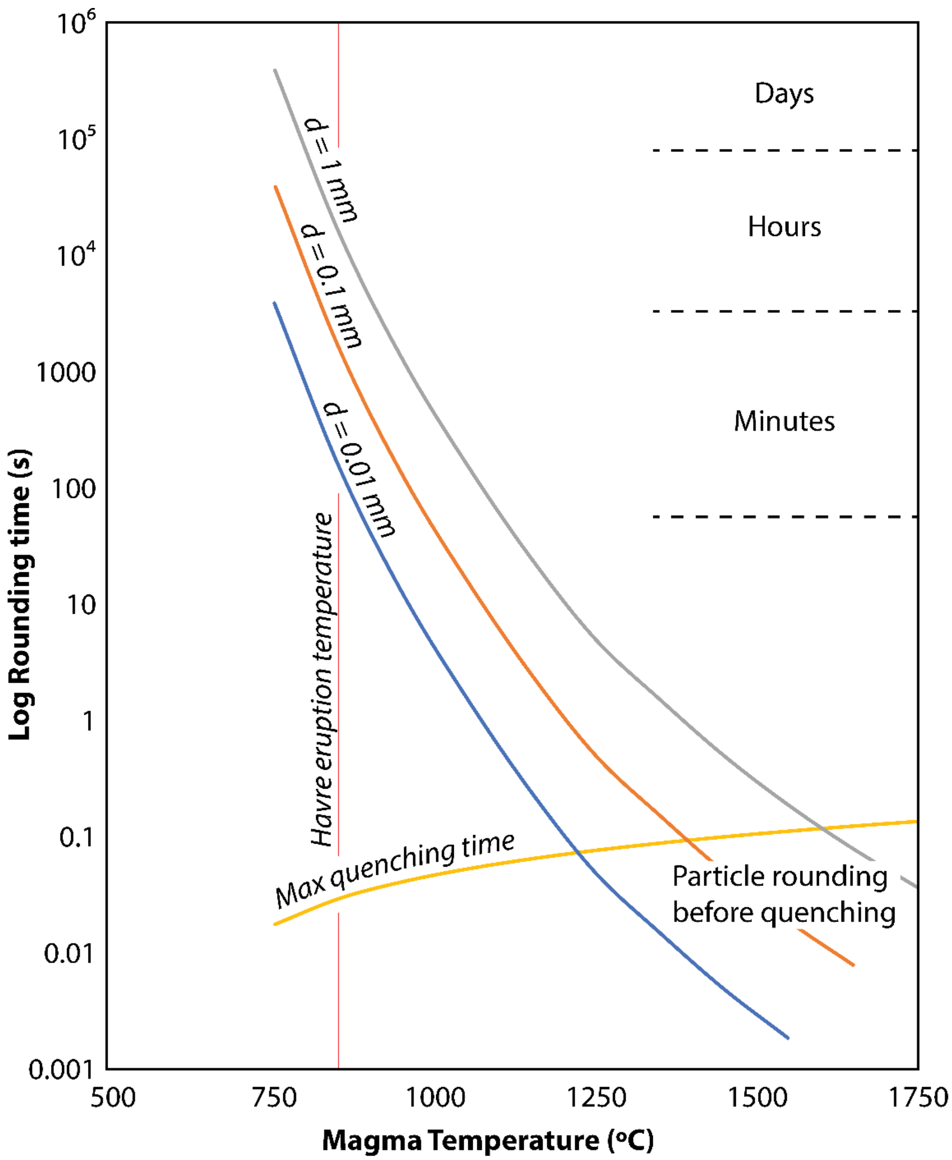

There are several limitations involved in this analysis. Cooling rate dependence of the glass transition temperature produces variation of approximately 80 K, for cooling rates of between 0.000017-0.105 K s^{-1} (Gottsmann and Dingwell, 2001, 2002). In addition, particle cooling from the outside rim in would restrict surface tension rounding processes first therefore lowering quenching timescales in the natural environment. Ash particles are also likely to have cooled from the eruption temperature following fragmentation. The timescale presented here therefore represents an upper limit to the quenching timescale experience by the Havre ash on contact with water.

References cited

Carey, R., Adam Soule, S., Manga, M., White, J.D.L., McPhie, J., Wysoczanski, R., Jutzeler, M., Tani, K., Yoerger, D., Fornari, D., Caratori-Tontini, F., Houghton, B., Mitchell, S., Ikegami, F., et al., 2018, The largest deep-ocean silicic volcanic eruption of the past century: Science Advances, v. 4, doi: 10.1126/sciadv.1701121.

Gardner, J.E., and Ketcham, R.A., 2011, Bubble nucleation in rhyolite and dacite melts: Temperature dependence of surface tension: Contributions to Mineralogy and Petrology, v. 162, p. 929–943, doi: 10.1007/s00410-011-0632-5.

Giordano, D., Russell, J.K., and Dingwell, D.B., 2008, Viscosity of magmatic liquids: A model: Earth and Planetary Science Letters, v. 271, p. 123–134, doi: 10.1016/j.epsl.2008.03.038.

Gottsmann, J., and Dingwell, D.B., 2001, The cooling of frontal flow ramps: A calorimetric study on the Rocche Rosse rhyolite flow, Lipari, Aeolian Islands, Italy: Terra Nova, v. 13, p. 157–164, doi: 10.1046/j.1365-3121.2001.00332.x.

Gottsmann, J., and Dingwell, D.B., 2002, The thermal history of a spatter-fed lava flow: The 8-ka pantellerite flow of Mayor Island, New Zealand: Bulletin of Volcanology, v. 64, p. 410–422, doi: 10.1007/s00445-002-0220-7.

Gottsmann, J., Giordano, D., and Dingwell, D.B., 2002, Predicting shear viscosity during volcanic processes at the glass transition: A calorimetric calibration: Earth and Planetary Science Letters, v. 198, p. 417–427, doi: 10.1016/S0012-821X(02)00522-8.

Helo, C., Clague, D.A., Dingwell, D.B., and Stix, J., 2013, High and highly variable cooling rates during pyroclastic eruptions on Axial Seamount, Juan de Fuca Ridge: Journal of Volcanology and Geothermal Research, v. 253, p. 54–64, doi: 10.1016/j.jvolgeores.2012.12.004.

Newman, S., and Lowenstern, J.B., 2002, Volatile Calc : a silicate melt – $H2O$ – $CO2$ solution model written in Visual Basic for excel: Computers & Geosciences, v. 28, p. 597–604, doi: doi:10.1016/S0098-3004(01)00081-4.

Wadsworth, F.B., Vasseur, J., Llewellin, E.W., Genareau, K., Cimarelli, C., Dingwell, D.B., Vesseur, J., Llewellin, E.W., Genareau, K., Corrado, C., and Dingwell, D.B., 2017, Size limits for rounding of volcanic ash particles heated by lightning: Journal of Geophysical Research: Solid Earth, v. 122, p. 1977–1989, doi: 10.1002/2016JB013864.

DR 5 Conduit wall viscous heating rate at Havre

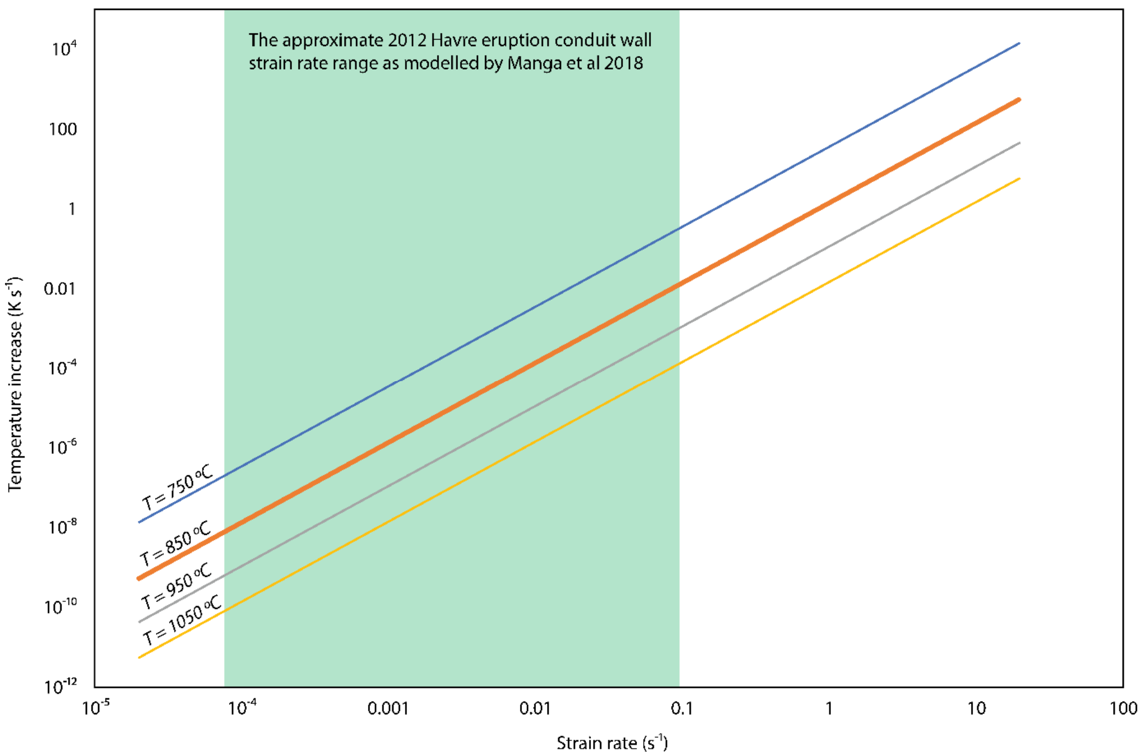

The rate of viscous heating (dT/dt) for the Havre magma over a range of temperatures and a range of strain rates (γ') calculated using equation (6) from Hess et al. (2008).

$$\frac{dT}{dt} = \frac{\mu \cdot \gamma'^2}{\rho \cdot C_p}$$

Where μ is the magma viscosity, ρ is the magma density here assumed to be 2300 kg m^{-3}, and C_p is the magma heat capacity. Conduit margin strain rates predicted by (Manga et al., 2018) during the Havre eruption range between ~10^{-4} to 10^{-1} s^{-1} producing negligible viscous heating at the estimated eruption temperature (850 ^{o}C).

References cited

Hess, K.U., Cordonnier, B., Lavallée, Y., and Dingwell, D.B., 2008, Viscous heating in rhyolite: An in situ experimental determination: Earth and Planetary Science Letters, v. 275, p. 121–126, doi: 10.1016/j.epsl.2008.08.014.

Manga, M., et al., 2018, The pumice raft-forming 2012 Havre submarine eruption was effusive: Earth and Planetary Science Letters, v. 489, p. 49–58, https://doi.org/10.1016/j.epsl.2018.02.025.